Food Chemistry: X 15 (2022) 100379

Contents lists available at ScienceDirect

Food Chemistry: X

journal homepage: www.sciencedirect.com/journal/food-chemistry-x

Insights into a new alternative method with graphene oxide/polyacrylamide/Fe_3O_4 nanocomposite for the extraction of six odor-active esters from Strong-aroma types of Baijiu

Ling Ao [a,b,d], Xudong Lian [a,b], Wenxuan Lin [b,c], Ruonan Guo [a,b], Youqiang Xu [b,c], Wei Dong [a,b,*], Miao Liu [d], Caihong Shen [d], Xiaotao Sun [a,b], Baoguo Sun [a,b,c], Bo Deng [d]

[a] Key Laboratory of Brewing Molecular Engineering of China Light Industry, Beijing Technology and Business University, Beijing 100048, PR China
[b] Beijing Laboratory of Food Quality and Safety, Beijing Technology and Business University, Beijing 100048, PR China
[c] Beijing Advanced Innovation Center for Food Nutrition and Human Health, Beijing Technology and Business University, Beijing 100048, China
[d] Luzhou Laojiao Co. Ltd., Luzhou, Sichuan 646000, PR China

ARTICLE INFO

Keywords:
Magnetic solid phase extraction
Graphene oxide/polyacrylamide/Fe_3O_4
Adsorption behavior
Alternative method
Odor-active esters
Strong-aroma types of Baijiu

ABSTRACT

Liquid-liquid extraction (LLE) is the most commonly utilized technique for the extraction of odor-active esters (OAEs) in strong-aroma types of Baijiu (SAB). However, since the contents of different OAEs in SAB vary widely, it is still a puzzle to ensure that all OAEs to be thoroughly extracted by LLE without the problem of saturated adsorption. Herein, a novel approach of magnetic solid phase extraction (MSPE), based on the magnetic graphene oxide nanocomposite modified with polyacrylamide (GO/PAM/Fe_3O_4), was employed for the efficient extraction of six OAEs from SAB. Compared with LLE, GO/PAM/Fe_3O_4 exhibited highly selective recognition properties and larger adsorption capacities for OAEs (ranging from 13.68 to 39.06 mg/g), resulting in better extraction performances for OAEs. Coupled with GC–MS, six OAEs in real SAB were successfully determined, with recoveries ranged from 70.1 ~ 90.0% and LODs at 0.08 ~ 1.35 μg/L. Overall, the MSPE-GC/MS is a promising alternative for accurate determination of OAEs in SAB.

Introduction

Strong-aroma types of Baijiu (SAB), which account for approximately 70% of the total Baijiu consumption, are among the foremost traditional distillates in China (Liu & Sun, 2018). In decades, numerous studies have demonstrated that aroma is one of the most important indicators that contribute to SAB quality and consumer acceptance. At present, more than 860 volatile compounds have been determined in SAB; moreover, new compounds continue to emerge with more advanced analytical techniques. Among them, 32 odorants proved to be the key compounds responsible for the unique aroma characteristics of SAB, with the aid of gas chromatography − olfactometry, quantitative measurement and flavor contribution analysis (J. Wang, Chen, Wu, & Zhao, 2022). Esters, which are mainly made by the esterification of alcohols and fatty acids, are among the foremost aroma components in strong-aroma types of Baijiu (SAB). According to the latest statistical data summarized by our group, esters achieved the highest proportion of the total mass of flavor substances in SAB, accounting for almost 30% (Sun, 2021). Nowadays, thanks to their lower odor threshold values, most of esters were regarded as the odor-active compounds and contribute greatly to the odors of SAB (Dong et al., 2019). Furthermore, many of these odor-active esters (OAEs) can also enrich the taste of baijiu together with acids, aldehydes and alcohols (Xu et al., 2022). Therefore, an accurate determination of OAEs plays a vital role in revealing its influence on the flavor of Baijiu.

Owing to the trace level of OAEs in SAB, a sample-preparation step is required to extract and enrich the target analytes prior to the instrumental analysis. Previously reported extraction methodologies of OAEs from SAB have mainly included liquid–liquid extraction (LLE), solid-phase microextraction (SPME), stir bar sorptive extraction (SBSE) and solid-phase extraction (SPE) (He, Yangming, Górska-Horczyczak, Wierzbicka, & Jeleń, 2021; Niu, Yu, Xiao, Zhu, Song, & Zhu, 2015; Zhao et al., 2018). Among them, LLE has become the most commonly utilized technique for the extraction of OAEs in SAB. However, the main drawbacks of LLE are as follows: (i) The principle that “like dissolves like” is used for the extraction of target analytes from sample during LLE. But

* Corresponding author at: College of Light Industry, Beijing Technology and Business University, Beijing 100048, PR China.
E-mail address: 20200812@btbu.edu.cn (W. Dong).

https://doi.org/10.1016/j.fochx.2022.100379
Received 4 April 2022; Received in revised form 19 June 2022; Accepted 25 June 2022
Available online 28 June 2022

the "impurities" with the same polarity can also be extracted when using organic solvents (e.g., dichloromethane, carbon tetrachloride, and *n*-hexane) for target esters extraction, leading to the excessively high background signal and false-negative results (unpublished data). (ii) The contents of different esters in SAB vary widely, ranging from tens of ppb to even hundreds of thousands of ppm, it is still a puzzle to ensure that all the above-mentioned esters to be thoroughly extracted by LLE without the problem of saturated adsorption. (iii) The operation of LLE is still complicated and time-consuming, since a series of steps such as sample dilution, extraction, drying, evaporation and redissolution were required to complete the preprocessing (Du et al., 2021). Hence, developing more simple, rapid, and efficient method for ester pretreatment is still of great value and demand.

Compared with traditional pretreatment technologies, magnetic solid phase extraction (MSPE) has received increasing attention in trace analysis owing to its easy operation, excellent adsorption efficiency, rapid separation, and good reusability (Zhang, Liu, Cao, Yin, & Zhang, 2020). Recently, many studies have demonstrated that the functional modification for different targets can increase the extraction efficiencies of the targets and widen the application of MSPE. Notably, a variety of materials have been used to modify magnetic nanoparticles (MNPs) and used as sorbents for MSPE such as carbon materials, organic polymer, organic skeleton compounds and graphene oxide (Karbalaie, Rajabi, & Fahimirad, 2020). Among them, MSPE based on the magnetic graphene oxide microsphere (Fe_3O_4/GO) has been demonstrated to be an effective approach for the extraction of ester compounds in food matrices. For instance, on account of its special nanostructures with huge specific surface area and good thermal/chemical stability, Fe_3O_4/GO nanocomposite has been used to enrich three ester compounds from food samples by Xiao et al (Xiao et al., 2017). Moreover, Yin et al. successfully synthesized and applied three MNPs, including magnetic multiwalled carbon nanotubes (Fe_3O_4/MWCNTs), Fe_3O_4 and Fe_3O_4/GO, for the determination of eleven PAEs in four beverages, combined with HPLC (Yin et al., 2019). However, until now, it has yet to be emphasized that only magnetic particles modified with GO were deficient owing to their poor dispersion in the tested sample solutions (Guo et al., 2019).

Polyacrylamide (PAM) hydrogels are a kind of hydrophilic polymer, which have a high specific surface area and many tertiary and primary amine groups in their inner and surface structure (Viana et al., 2020). Due to its abundant amine groups, the PAM hydrogel can not only easily adsorb organic compounds with O- or *N*-containing functional groups through strong hydrogen bonds, but also, when PAM was introduced into GO, the COOH group of GO could protonate the $-NH_2$ group of PAM to form $NH_3^+\cdots COO^-$ ion pairs, which partly prevented the stacking of GO sheets, resulting in effective enhancement of the adsorption efficiency for the target analytes (Cheng et al., 2019). Currently, PAM hydrogels have been reported to significantly assist GO self-assembly into three-dimensional (3D) graphene macrostructures and improve the adsorption ability of heavy metal ions and dyes from aqueous solutions at the same time (C. Dong, Lu, Qiu, Shen, Xing, & Zhang, 2018; Peng, Zhang, Huang, Jin, & Peng, 2019). OAEs (Fig. S1) are compounds with −COO− groups. The chemical structures of OAEs make them good candidates for MSPE extraction thanks to the presence of the –COO–groups, which provides a strong H-bonding with the $–NH_2$ groups of GO/PAM. Furthermore, if the advantages of Fe_3O_4 could be combined in perfection, it would allow a more effective extraction of OAEs from SAB through additional electrostatic interactions. However, no relevant work has been reported dealing with the application of GO@PAM@-Fe_3O_4 for the extraction of OAEs from SAB.

Given all this, the purpose of this work was to (i) synthesize a novel polyacrylamide-functionalized magnetic graphene oxide (GO/PAM/Fe_3O_4) material by a one-step radical polymerization and in situ chemical coprecipitation strategy and apply it to the extraction of six OAEs from SAB, (ii) illustrate the adsorption behavior and mechanism of GO/PAM/Fe_3O_4 towards six OAEs through adsorption isotherms and kinetics, and (iii) accurately quantitate six OAEs in SAB by means of isotope internal standards followed by the calculation of OAVs and thus further verify the contribution of these esters to the SAB.

Materials and methods

Chemicals and reagents

GO (98.0%) with a thickness of 0.7 ~ 1.2 nm and sodium chloride (99.5%) were purchased from Yuanye Biological Reagent Co., Ltd. (Shanghai, China). Acrylamide (AM, 99.0%), ammonium persulfate (APS, 98.0%), N, N'-methylene bisacrylamide (MBA, 98.0%), sodium hydroxide (NaOH, ≥ 96.0%), HPLC-grade dichloromethane (CH_2Cl_2, 99.9%), acetone (99.7%), ethyl acetate (99.9%), tetrachloromethane (CCl_4, 99.5%), hexane (99.7%), and HCl solution (36.0%~38.0%) were obtained from J&K Scientific Ltd. (Beijing, China). $FeCl_3{\cdot}6H_2O$ (99.5%), $FeCl_2{\cdot}4H_2O$ (99.95%), and ammonium solution (≥25.0% in H_2O) were purchased from Aladdin Reagents Co., Ltd. (Shanghai, China). Ultrapure water was prepared through a Milli-Q system at 18.2 MΩ (Millipore, Bedford, MA).

The standards of ethyl pentanoate, ethyl hexanoate, propyl hexanoate, butyl hexanoate, ethyl octanoate, and hexyl hexanoate, with purities over 99%, were purchased from J&K Scientific Co., Ltd. (Beijing, China). $^2H_5$-Ethyl pentanoate (IS1, ≥ 95%) and $^2H_5$-propyl hexanoate (IS2, ≥ 95%) were used as isotope internal standards and obtained from Yuanye Biological Reagent Co., Ltd. (Shanghai, China). The stock standard solutions of each compound were prepared in ethanol and stored at 4 °C until analysis. A freshly prepared ethanol–-water solution at 15% alcohol by volume (ABV) was used as a synthetic model of Baijiu.

Preparation of GO/PAM/Fe_3O_4 nanocomposites

Synthesis of GO/PAM hydrogel

The GO/PAM hydrogel was synthesized by a one-pot free-radical polymerization (Peng et al., 2019). Typically, 30 mg of graphite powder was dispersed in a centrifuge tube containing 7.5 mL Milli-Q water and ultrasonicated for 1 h to exfoliate the GO. Subsequently, 1 g of AM, 7.5 mL of APS (44.0 mg/mL) and 0.02 g of MBA cross-linker were dissolved in the aforementioned GO solution and transferred to a 100 mL round bottom flask equipped with a condenser, a thermometer, and a magnetic stirrer. Then, the as-prepared mixture was stirred vigorously at 200 r/min. The GO/PAM hydrogels were eventually formed after reacting for 8 h at 63 °C. To dehydrate the aforementioned gel, GO/PAM was cut into 1 cm^3 cubes before being washed with ultrapure water to pH 7.0; the water was replaced every 3 h to remove unreacted monomers and other impurities. Finally, the GO/PAM was dried in a −50 °C vacuum freeze drier for over 48 h (Fig. S2A).

Synthesis of GO/PAM/Fe_3O_4

A chemical coprecipitation method was used for the magnetization of the synthesized GO/PAM because of its easy application and high-volume capability. This method is based on the coprecipitation of water-soluble Fe^{2+} and Fe^{3+} ions in a basic medium. As shown in Fig. S2B, $FeCl_3{\cdot}6H_2O$ (0.5406 g) and $FeCl_2{\cdot}4H_2O$ (0.1988 g) were dissolved in 20.0 mL of HCl solution (0.4 M) and transferred to a 250.0 mL round bottom flask. After a 15.0 min ultrasonic dispersion treatment at 35 °C, 0.21 g of the as-prepared GO/PAM was well dispersed in 20.0 mL ultrapure water. Then, this dispersion was added dropwise into the $FeCl_2$/$FeCl_3$/HCl solution and stirred with a magnetic stirrer at room temperature for 1 h. After stirring, 160.0 mL of a 1.25 M ammonia solution were added dropwise at a rate of 10 d/min to adjust the solution *p*H ranging from 10 ~ 12 to the solution, and then the aforementioned reaction was stirred vigorously at 90 °C for 4 h. After magnetic particles formed, the as-prepared mixture was washed with ultrapure water until pH 7.0, separated with a neodymium magnet several times to remove the residual GO/PAM, and then dried in a 60 °C oven for approximately

12 h.

Characterization of the GO/PAM/Fe_3O_4

The morphologies and dimensions of the synthesized materials were analyzed using scanning electron microscopy (SEM, Hitachi Su-8020, Tokyo, Japan). A Fourier transform infrared (FT-IR) spectrometer (AVATAR-370 FT-IR, Thermo Nicolet, Waltham, MA) in the range of 400 ~ 4000 cm^{-1} was applied to characterize the sorbents mentioned above. The crystal structural analysis of the as-prepared materials was carried out on an D8 Advance X-ray diffractometer (Brooke, Germany), using Cu Kα radiation over the angular ranging from 5° to 80°. X-ray photoelectron spectroscopy (XPS) was performed using a Thermo ESCALAB 250 Xi spectrometer with an Al Kα X-ray source ($h\upsilon = 1486.6$ eV). The magnetic properties of GO/PAM/Fe_3O_4 were analyzed with a vibrating sample magnetometer (Squid-VSM, Quantum Design, USA) at 27 °C by cycling the field between −50 and 50 kOe. Zeta potential measurements for GO and GO/PAM/Fe_3O_4 were determined on a Zetasizer Nano ZS90 (Marlven Instruments, United Kingdom).

Optimization of the MSPE conditions

To obtain the best adsorption efficiency of GO/PAM/Fe_3O_4 for extracting OAEs, several crucial parameters that may affect the performance of MSPE investigated, including (a) the amount of sorbent (10, 20, 30, 40 and 50 mg), (b) ionic strength (0, 0.1, 0.5, 2.0 and 4.0 mol/L), (c) the pH value of the sample solution (2, 4, 6.5, 8, 10), (d) extraction time (5, 10, 15, 20 and 30 min), and (e) desorption solvent (acetone, ethyl acetate, CH_2Cl_2, CCl_4 and hexane). The extraction efficiency of the developed adsorbent was evaluated from the enrichment factors (EFs) achieved by spiking six standard OAEs in synthetic SAB sample to obtain the final concentration of 2.0 mg/L. The EFs of six OAEs were defined as follows:

$$EF(\%) = Cd/C0 \times 100 \quad (1)$$

where C_d is the concentrations of six OAEs in the desorption solution after MSPE extraction, and C_0 is the initial concentration for the analyte in the synthetic SAB sample (2.0 mg/L).

Sample preparation and MSPE procedure

Sample preparation

Five SAB samples originating from Luzhoulaojiao Distillery Co., Ltd. (Sichuan Province, P. R. China) were used in this work and labeled SAB-1, SAB-2, SAB-3, SAB-4, and SAB-5. The aforementioned SAB samples were all prepared by dissolving them in 15% ABV with ultrapure water; the pH of the final sample solution was adjusted to 6.5 with 0.1 M NaOH and then subjected to the MSPE procedure.

Magnetic solid phase extraction procedure

For the MSPE procedure, 5.0 mL of the adjusted SAB solution was loaded into a 10.0 mL centrifuge tube. Then, the samples were spiked with the respective isotopically labeled internal standards to give final concentrations of 20.0 mg/L and saturated with NaCl. Next, 10.0 mg of GO/PAM/Fe_3O_4 was dispersed in the aforementioned sample solution, and the mixture was shaken by IKA VORTEX 2 vortex agitators at 2800 rpm for 15.0 min to reach adsorption equilibrium. Subsequently, an external magnet was attached at the side of the centrifuge tubes to separate the GO/PAM/Fe_3O_4 with the adsorbed analyte from the solution. Thereafter, 0.5 mL of CCl_4 was added and ultrasonicated for 15 min at 40 °C to elute the analytes from the adsorbents. Finally, a 1.0 μL aliquot of eluate was injected into the GC–MS system for analysis.

GC–MS analysis of OAEs

Six OAEs were quantified by GC–MS (Trace 1300 GC-ISQ LT GC–MS system, Thermo Fisher Scientific, Waltham, MA). The chromatographic separation was achieved on a DB-WAX capillary column (30 m × 0.25 mm, 0.25 μm film thickness, Agilent Technologies, Palo Alto, CA) using helium (99.999%) as carrier gas with a constant flow rate of 1.0 mL/min. The front inlet was performed with a split ratio of 10:1 at 250 °C for MSPE (1.0 μL injected). The oven temperature was initially held at 45 °C, then raised to 80 °C at 10 °C/min and held for 5.0 min, finally ramped at the rate of 10 °C/min to 245 °C and held for 2.0 min. For the MS conditions, the temperatures of the transfer line and ionization source were 240 °C and 230 °C, respectively. The mass spectra were collected in electronic impact mode (EI, 70 eV voltage), and the acquisitions were performed over a *m/z* scan range of 45 to 450 amu at 0.2 s intervals. A selected ion monitoring (SIM) mode was used in MS analysis during OAEs quantification and the ions for both unlabeled and labeled ethyl pentanoate, ethyl hexanoate, propyl hexanoate, butyl hexanoate, ethyl octanoate and hexyl hexanoate resulted in values of 89, 88, 88, 104, 99, 56, 88, and 117 (detailed in Table S1).

Adsorption mechanism studies

Batch experiments were performed to evaluate the adsorption characteristics of six OAEs with an optimum pH (6.5) and at room temperature (298 K, 25 °C). 10.0 mg of the GO/PAM/Fe_3O_4 sorbent was added to 5.0 mL of a mixed ester solution with concentrations ranging from 10.0 ~ 100.0 mg/L, and the mixture was subjected to constant agitation (180 rpm) at 25 °C. After adsorption, the ester-loaded adsorbents were magnetically separated from the solution at intervals of 5, 10, 15, 40, 60, 90 and 120 min. Finally, the amounts of six OAEs in the filtrate were determined according to previous methods with modifications (Dong et al., 2019) and are detailed in the Supplementary data. The adsorption capacities for the aforementioned OAEs were expressed as Q_t (mg/g) at time t and calculated using the following equation:

$$Qt = (C0 - Ct)V/m \quad (2)$$

where C_0 and C_t (mg/L) are the concentrations of the six OAEs at the initial time and time t, respectively; V (mL) is the volume of the tested solution; and m (mg) is the weight of GO/PAM/Fe_3O_4.

Statistical analysis

All chemical analyses in this work were carried out in triplicate, and the results are reported as the mean ± standard deviation (SD). Significant differences among samples were estimated by employing one-way analyses of variance (ANOVA) and unpaired Student's t-tests. F-tests and p-values were calculated using SPSS software ver. 19.0 (IBM Co., Armonk, NY, USA). The means were considered significantly different at a p-value < 0.05 (Table S2).

Results and discussion

Characterization of GO/PAM/Fe_3O_4

As shown in Fig. 1A, GO has a transparent sheet structure with a rough surface and contains some wrinkles, which could potentially improve the interaction with Fe_3O_4 and PAM chains. After functionalization of GO with PAM (shown in Fig. 1B), it is clear that the PAM flake crystals successfully assembled on the graphene oxide nanosheet (Ploychompoo, Liang, Zhou, Wei, & Luo, 2021). In addition, as shown in Fig. 1C, the surface of GO/PAM/Fe_3O_4 was homogeneously covered with monodisperse Fe_3O_4 spheres and partially aggregated Fe_3O_4, resulting in GO/PAM/Fe_3O_4 having a rougher surface than GO/PAM. The above result demonstrated that the GO sheets were eventually uniformly coated with Fe_3O_4 and PAM particles (Senosy, Guo, Ouyang, Lu, Yang, & Li, 2020).

XRD measurements were employed to identify the crystalline phase and structure of GO, GO/PAM and GO/PAM/Fe_3O_4. As shown in Fig. 1D,

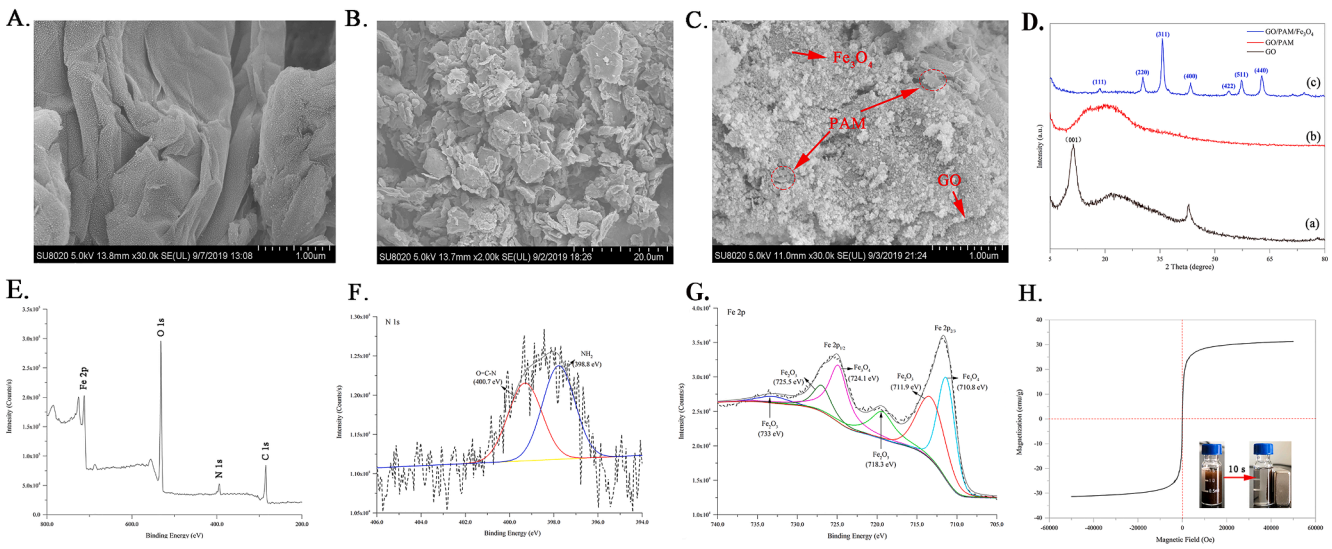

Fig. 1. (A-C) SEM image of GO, GO/PAM, and GO/PAM/Fe_3O_4; (D) XRD patterns of (a) GO, (b) GO/PAM, and (c) GO/PAM/Fe_3O_4; XPS spectra of GO/PAM/Fe_3O_4: (E) wide scan, (F) N1s, and (G) Fe2p; (H) VSM of the GO/PAM/Fe_3O_4.

a sharp diffraction peak at the 2θ position of 11.4°, which is indexed to the (0 0 1) plane of GO (Manousi, Deliyanni, Rosenberg, & Zachariadis, 2021). The GO/PAM hydrogel presented a broad non-crystalline diffraction region between 10° and 29°, indicate the successful impregnation of the PAM into the graphite oxide layers. In terms of GO/PAM/Fe_3O_4, seven peaks appeared at 2θ values of 18.4°, 30.2°, 35.7°, 43.4°, 53.8°, 57.2°, and 62.7°, which are characteristic peaks of Fe_3O_4, are attributed to the (1 1 1), (2 2 0), (3 1 1), (4 0 0), (4 2 2), (5 1 0), and (4 4 0) planes, respectively (Filho, Brito, Silva, Streck, Bohn, & Fonseca, 2021). However, it must be noted that the sharp characteristic peak of GO (2θ of 11.4°) did not appear in both GO/PAM and GO/PAM/Fe_3O_4 nanocomposite which attributed to either the complete exfoliation of GO sheets in the polymer or the partial exfoliation leaving a small amount of crystalline GO.

To further evaluate the functionalization of PAM and Fe_3O_4 on the surface of GO, XPS measurements of GO/PAM/Fe_3O_4 were obtained. As shown in Fig. 1E, the scan XPS spectra of the aforementioned nanocomposite appeared at binding energies of approximately 285, 532, 398, and 712 eV attributed to C1s, O1s, N1s, and Fe2p, respectively. Among them, the detection of the new characteristic peaks of N1s and Fe2p indicated that the PAM and magnetic particles successfully covered the GO/PAM/Fe_3O_4 surface. For instance, as shown in Fig. 1F, two peaks were present in the N1s spectrum of the aforementioned nanocomposite, which were attributed to NH_2 (amine) at 398.8 eV and O═C-N (amide) bonds at 400.7 eV in the grafted PAM. Furthermore, in the spectrum of Fe2p (Fig. 1G), the peaks at 724.1 and 710.8 eV correspond to the Fe2p1/2 and Fe2p3/2 of Fe_3O_4. However, it must be emphasized that Fe_2O_3 nanoparticles also existed on the GO/PAM/Fe_3O_4 surface due to the deconvolution result of the Fe2p spectrum: the peaks at 724.1 eV (Fe2p1/2) and 710.8 eV (Fe2p3/2) were attributed to Fe_3O_4, while the peaks at 733.0 eV (satellite), 725.5 eV (Fe 2p1/2), 718.3 eV (satellite) and 711.9 eV (Fe 2p3/2) belonged to Fe_2O_3. Apart from that, the deconvolution of the C1s peaks of GO/PAM/Fe_3O_4 is represented in Fig. S3A. The binding energy of 284.3 eV corresponded to C═C, the epoxy (C-OH) and alkoxyl carbon (C—O—C) and the carbonyl carbon (C═O) were 285.7 eV and 288.1 eV, respectively. Moreover, four types of oxygen species contributed to the O1s peak (Fig. S3B), that is, the contribution of the C═O bond was at 534.2 eV, the C—O was at 532.7 eV, and the hydroxyl group was at 531.2 eV. The peak at 529.3 eV is due to the contribution of the anionic oxygen in Fe_3O_4 (Fe-O) (Z. Lu, Yu, Zeng, & Liu, 2017).

The magnetic properties of the as-prepared GO/PAM/Fe_3O_4 were verified by the magnetization curve measured by VSM. As shown in Fig. 1H, the magnetic hysteresis loops of the aforementioned sorbent showed almost zero coercivity and remanence, which demonstrated that the synthesized GO/PAM/Fe_3O_4 possessed superparamagnetic properties with a saturated magnetization value of 31.3 emu/g. After the extraction step, the sorbent prepared in this study could be easily separated from the tested SAB sample within 10 s using an external magnet (shown in the inset in Fig. 1H). These results indicated that the as-prepared GO/PAM/Fe_3O_4 was suitable as an absorbent for the MSPE process.

Optimization of the MSPE conditions

Effect of the adsorbent amount

The amount of magnetic adsorbent added seems to directly connect with the quantity of adsorbed analytes and to affect the extraction efficiency; therefore, to optimize the GO/PAM/Fe_3O_4 amount, a series of amounts (10.0 ~ 50.0 mg) were added to the sample solution. As shown in Fig. 2A, the maximum extraction efficiency of six OAEs was achieved when only 10.0 mg of the aforementioned sorbent was used. However, with a further increase in the quantity of the tested sorbent from 10.0 to 50.0 mg, the extraction efficiencies of esters remained stable. This might be due to aggregation between GO/PAM/Fe_3O_4, leading to a reduction in the effective adsorption surface area. Therefore, 10.0 mg of GO/PAM/Fe_3O_4 was chosen for the subsequent study.

Effect of ionic strength

The influence of ionic strength on the extraction efficiencies of six OAEs was investigated by changing the sodium chloride (NaCl) concentration from 0 ~ 4.0 mol/L (saturated). As shown in Fig. 2B, the EFs of the six OAEs increased significantly ($p = 0 \sim 2.45 \times 10^{-5}$, shown in Table S2) with increasing NaCl concentration from 0 to 4.0 mol/L. This might be explained by the salting-out effect. Generally, the addition of salt would decrease the solubility of target OAEs in the aforementioned synthetic model of SAB, which led to an enhancement of the adsorption efficiency of analytes onto GO/PAM/Fe_3O_4 (Senosy et al., 2020). Therefore, 4.0 mol/L NaCl was added for further study.

Effect of the sample pH

The pH of the sample solution is crucial to the extraction efficiency of six OAEs, as it would affect the existing forms of targets, the charged species, and the density of the GO/PAM/Fe_3O_4 surface. In this work,

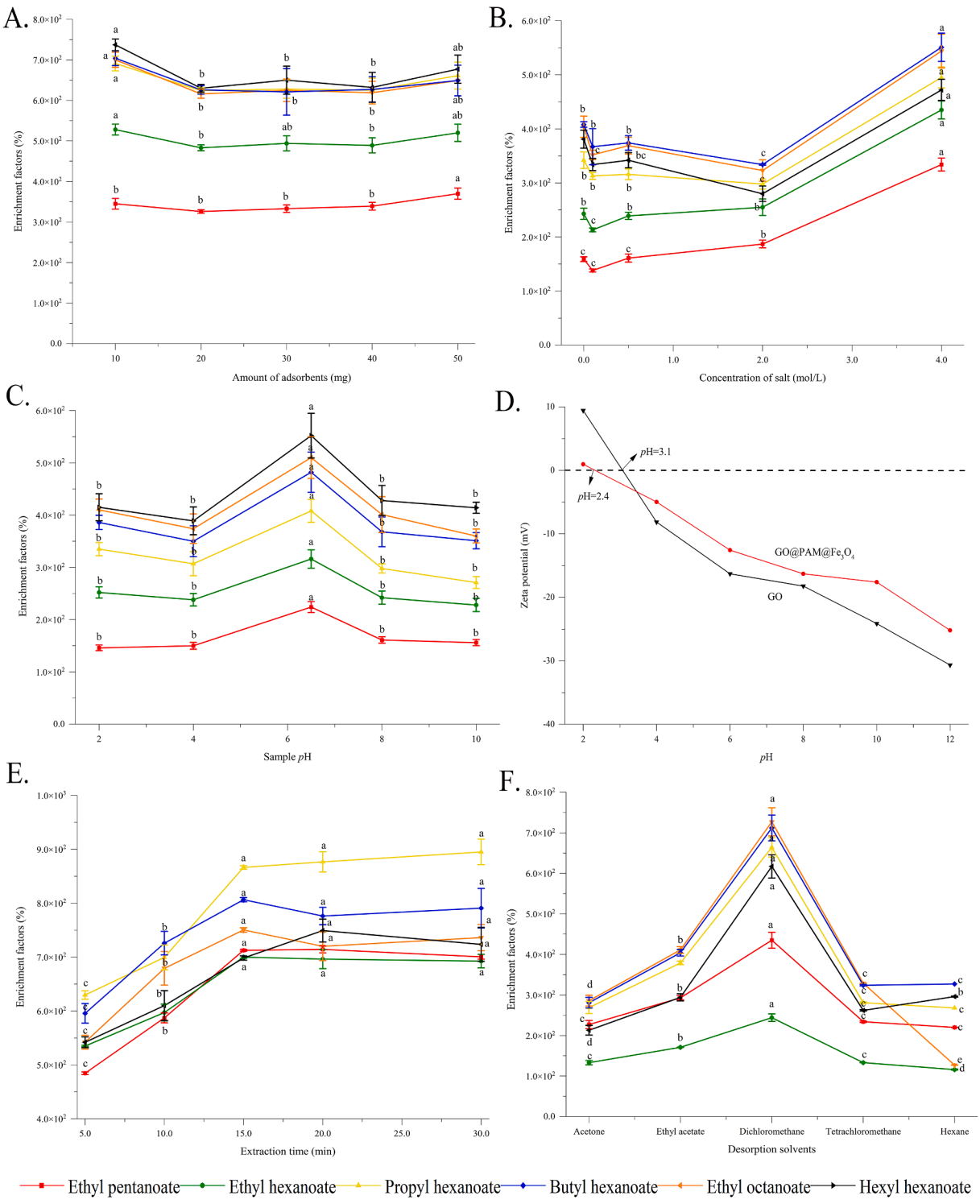

Fig. 2. Effect of (A) the amounts of adsorbents, (B) salt additions, (C) the sample pH, (E) extraction time, and (F) type of desorption solvent on the extraction efficiency of six OAEs using GO/PAM/Fe_3O_4; (D) ζ-potential of GO (in black) and GO/PAM/Fe_3O_4 (in red) at pH values ranging from 2.0 to 12.0.

Fig. 2C shows the effect of pH values ranging from 2.0 to 10.0 on the adsorption capacity of the six esters. The optimized adsorption efficiency (enrichment factors, EFs ranging from 224.0 ~ 552.0%) was achieved when the pH was adjusted to 6.5. The following reasons might explain this observation. (i) Esters are known to undergo reversible or irreversible hydrolysis reactions in acidic or alkaline conditions, leading to the formation of an acid and an alcohol or a carboxylate and an alcohol, respectively (Eq. (3)) (Zhan, Landry, & Ornstein, 2000). More importantly, the aforementioned reaction could easily occur when the pH was in the range of 2 ~ 4 or above 10. Therefore, as shown in Fig. 2C, when the pH decreased from 4 to 2 or increased from 8 to 10, the extraction efficiencies of the six OAEs declined as a whole.

$$RCOOR' + H2O \rightleftharpoons RCOOH + R'OH(H + condition)$$

$$RCOOR' + OH^- \rightleftharpoons RCOO^- + R'OH(OH - condition) \quad (3)$$

(ii) It could be speculated that the six OAEs were adsorbed on the

surface of GO/PAM/Fe_3O_4 mainly through hydrogen bonding. However, more oxygen-containing groups (such as –COOH and –OH) on the surfaces of the as-prepared sorbent were ionized as the pH increased from 4 to 10 (as seen in Fig. 2D, the point of zero charge of GO/PAM/Fe_3O_4 was at a pH of 2.4), which resulted in a gradual weakening of the electrostatic force between the analytes and the adsorbent; more importantly, the extraction efficiencies were significantly reduced as well ($p = 2.55 \times 10^{-4} \sim 0.021$, Table S2). Based on the results mentioned above, the optimum pH was employed at 6.5 for the subsequent experiments.

Effect of the extraction time

The effect of extraction time on the extraction efficiency of the six OAEs was studied by increasing the time from 5.0 to 30.0 min. As shown in Fig. 2E, partition equilibrium for all OAEs could be rapidly achieved within 15.0 min, with EFs ranging from 698.3 ~ 866.4%; however, the EFs of the aforementioned six analytes remained almost constant from 15.0 ~ 30.0 min. Therefore, 15.0 min was selected for the subsequent experiments. During the MSPE procedure, adsorption takes place in a short time, which indicates that the synthesized GO/PAM/Fe_3O_4 has a large surface area; hence, rapid mass transfer occurred between the adsorbents and the SAB solution.

Effect of desorption solvents

After the extraction step, the analytes adsorbed on the magnetic GO/PAM sorbent were desorbed using various organic solvents (including acetone, ethyl acetate, CH_2Cl_2, CCl_4 and hexane) under ultrasonication. As illustrated in Fig. 2F, the best EFs were obtained when CCl_4 was chosen as the desorption solvent. This is due to the polarity of the solvent, which largely determines the solubility of analytes. Since CCl_4 (partition coefficient, log P = 2.83) and the target analytes (log P = 2.2 ~ 4.76) have similar polarities, it can most effectively disrupt the interactions between the six OAEs and GO/PAM/Fe_3O_4, and can hence displace the analytes from the as-prepared sorbent. This phenomenon is consistent with the results described by numerous researchers (Dong et al., 2019). Consequently, CCl_4 was selected as the optimum eluent solvent.

Adsorption kinetics

Kinetic assessment is crucial to elucidate the path and mechanism as well as the rate of adsorption between target analytes and the adsorbent. In this study, the adsorption kinetics of GO/PAM/Fe_3O_4 for six OAEs were investigated at 298 K (25 °C) to determine the adsorption equilibrium time, and the results are shown in Fig. S4A. The uptake kinetics of the six OAEs were very rapid within 15 min and then increased slowly until adsorption equilibrium was reached. To elucidate the mechanism of adsorption, a pseudo-first-order (PFO) model and a pseudo-second-order (PSO) model were used to fit the kinetic data. Two models can be expressed as follows (Liang, Lu, Li, Li, & Zhu, 2020):

$$\text{PFO model}: \ln(Qe - Qt) = -k1t + \ln Qe \quad (4)$$

$$PSO\ model: \frac{t}{Qt} = \frac{1}{Qe}t + \frac{1}{k2Qe^2} \quad (5)$$

where Qt (mg/g) is the amount of adsorbed compounds at time t and Qe (mg/g) is the adsorption capacity of compounds at the equilibrium state. k_1 (1/min) and k_2 [g/(mg·min)] represent the adsorption rate constants of PFO and PSO, respectively.

As shown in Table 1, the slopes, intercepts, and correlation coefficients (R^2) of these plots are summarized. The high R^2 values for the PSO model (0.9992 ~ 0.9999) demonstrate that the model was better for describing OAEs adsorption by the GO/PAM/Fe_3O_4 sorbent (Fig. S4B). Moreover, the experimental results showed that the adsorption capacities *(Qe)* of the adsorbent for six OAEs were between 3.66 and 4.52 mg/g. Compared to those calculated by the PFO model, the PSO model predicted an appropriate theoretical *Qe* (3.58 to 4.46 mg/g) close to the experimental *Qe*. These results showed that adsorption mainly depends on the adsorption capacity of the surface position (Fraga et al., 2020).

Adsorption isotherms

Equilibrium studies were performed to determine the association among six OAEs concentration and amount of OAEs adsorbed at a constant temperature is usually recognized as adsorption isotherms study. In this work, the adsorption experiments of isotherms were conducted by changing the OAEs concentrations (10 ~ 100 mg/L, pH = 6.5) at 298 K. As observed from Fig. S4C, the absorptivity of six OAEs indicated that with increasing concentration, the amount of OAEs absorbed on GO/PAM/Fe_3O_4 also increased until reaching equilibrium. This phenomenon can be ascribed to that the active sites of GO/PAM/Fe_3O_4 are sufficient for six OAEs molecules occupation at the saturation concentration of OAEs, but has no ability to allow the extra OAEs molecules in the solutions with higher concentration.

In the interest of better evaluating the adsorption performance of GO/PAM/Fe_3O_4, the Langmuir (Eq.6) and Freundlich (Eq.7) isotherm models were used to simulate adsorption isotherm data (Pourjavadi, Nazari, Kohestanian, & Hosseini, 2019).

$$\text{Langmuir isotherm odel}: \frac{1}{\text{Qe}} = \frac{1}{\text{KLQmax}} \times \frac{1}{\text{Ce}} + \frac{1}{\text{Qmax}} \quad (6)$$

$$Freundlich\ isotherm\ model: \ln Qe = \frac{1}{n}\ln Ce + \ln Kf \quad (7)$$

where Q_e (mg/g) represents the adsorption capacity of esters at equilibrium; C_e (mg/L) is the concentration of OAEs in the synthetic model of SAB after reaching equilibrium; and Q_{max} (mg/g) denotes the

Table 1
Parameters of Langmuir, Freundlich, pseudo-first-order, and pseudo-second-order of six OAEs onto GO/PAM/Fe_3O_4.

Model	Equation and Parameters	Ethyl hexanoate	Ethyl pentanoate	Ethyl octanoate	Hexyl hexanoate	Propyl hexanoate	Butyl hexanoate
Pseudo-first-order kinetics	$Q_{e,\ exp}$ (mg g^{-1})	3.66	3.74	4.16	3.83	4.52	3.88
	$Q_{e,\ cal}$ (mg g^{-1})	1.14	0.96	0.95	0.95	1.03	0.84
	k_1 (g min^{-1} mg^{-1})	0.02	0.02	0.02	0.02	0.03	0.02
	R_1^2	0.5540	0.4907	0.4801	0.5066	0.6030	0.4531
Pseudo-second-order kinetics	$Q_{e,\ exp}$ (mg g^{-1})	3.66	3.74	4.16	3.83	4.52	3.88
	$Q_{e,\ cal}$ (mg g^{-1})	3.58	3.62	4.03	3.68	4.46	3.77
	k_2 (g min^{-1} mg^{-1})	0.25	0.22	0.44	0.99	0.48	0.26
	R_2^2	0.9994	0.9992	0.9997	0.9998	0.9999	0.9995
Langmuir isotherm	Q_{max} (mg g^{-1})	39.06	24.21	15.17	13.68	21.14	18.28
	K_L (L mg^{-1})	0.0041	0.0031	0.0180	0.0211	0.0205	0.0158
	R^2	0.9960	0.9943	0.9989	0.9967	0.9991	0.9956
	R_L	0.75 ~ 0.96	0.76 ~ 0.97	0.36 ~ 0.85	0.32 ~ 0.83	0.38 ~ 0.83	0.39 ~ 0.86
Freundlich isotherm	K_f (mg g^{-1})	0.3468	0.0796	0.5554	0.6395	0.9436	0.6197
	$1/n$	0.8613	1.0325	0.6400	0.5949	0.6116	0.6365
	R^2	0.9688	0.9545	0.9775	0.9552	0.9794	0.9494

maximum adsorption capacity. K_L is the Langmuir constant related to the adsorption energy; K_f and $1/n$ are the Freundlich constants; $1/n$ represents the degree of heterogeneity of the adsorbent surface.

As presented in Fig. S4D-S5 and Table 2, the adsorption behavior of GO/PAM/Fe3O4 for six OAEs follows the Langmuir model more than the Freundlich models. The regression coefficients (R^2) obtained using the Langmuir model (0.9943 ~ 0.9991) was higher than that calculated using the Freundlich equation (0.9494 ~ 0.9794). According to Langmuir model, the adsorption process on the surface of adsorbent done at specific homogeneous sites. No more adsorption process will proceed after the occupation of all available sites present on adsorbent molecule (Nazir et al., 2021). Therefore, these indicated that the adsorption of six OAEs occurred on the adsorbent's surface, and the adsorption process was a single-layer chemical adsorption process. Moreover. based on the Langmuir data, the Q_{max} values of six OAEs were calculated to range from 13.68 to 39.06 mg/g. Moreover, we calculated the separation factor R_L as the main characteristic of the Langmuir model using the Eq. (8).

$$RL = \frac{1}{1 + KLC0} \tag{8}$$

Based on the results of Table 1, the separation factor R_L of six OAEs ranges from 0.32 to 0.97, indicating the favorability of the adsorption of six OAEs by the novel proposed nanocomposite (Li et al., 2019).

Possible extraction mechanisms

It is well known that the chemical structures of the adsorbent play an important role in the adsorption phenomenon. In this work, the presence of active groups, such as amine, amide, hydroxyl, and carboxyl in the structure of GO/PAM/Fe_3O_4 might affect the tested OAEs adsorption. Considering its sensibility to the functional groups, the FT-IR spectra of GO/PAM/Fe_3O_4 before and after loading six OAEs were compared to gain insight into the adsorption mechanism.

In the FT-IR spectrum of GO/PAM/Fe_3O_4, shown in Fig. 3A, the peaks at 3370 cm^{-1}, 3193 cm^{-1} and 1580 cm^{-1}, which are related to the stretching vibrations of the N—H (or O—H) groups, and the bending vibration of the –NH_2 in GO/PAM/Fe_3O_4, shifted to 3330 cm^{-1}, 3170 cm^{-1}, and 1610 cm^{-1} after the adsorption of six OAEs, respectively, signifying that the H-bonding interaction occurred between the active sites of six OAEs and the amine groups and hydroxyls groups of GO/PAM/Fe_3O_4 (Hu et al., 2016). Besides, the carbonyl stretching peaks of six OAEs at 1735 cm^{-1} (curves i in Fig. 3B) disappeared and a new peak at 1658 cm^{-1} appeared (curves ii in Fig. 3B), which clearly indicated that the -COOR groups of the tested OAEs were connected with the amine groups in the surface modification of GO, forming -O-C═O···HN– hydrogen-bond (T. Lu, Xue, Shao, Gu, Zeng, & Luo, 2016). Based on the results mentioned above, the improvement in the adsorption efficiency between GO/PAM/Fe_3O_4 and the analytes was mainly dependent on hydrogen bonding.

Stability of the prepared GO/PAM/Fe_3O_4

The reusability and stability of GO/PAM/Fe_3O_4 for the adsorption of OAEs were tested in several successive runs, with the as-prepared sorbent being washed with 5 mL of CCl_4 and 5 mL of ultrapure water for three times and then dried in a vacuum oven at 60 °C for 6 h before the next use. The experimental results demonstrated that the adsorption feature of GO/PAM/Fe_3O_4 was apparently stable (<5%) after the repeated application of the above 5 cycles of sorption and desorption of the OAEs, indicating good reusability of the nanocomposite for ester adsorption.

Analytical performance of the proposed methods

Under the optimal conditions, the analytical properties of the established MSPE-GC/MS method were assessed by evaluating its linearity, LODs, LOQs, recoveries and precision. The calibration curves were constructed using the following equation: $y = ax + b$, where the peak area ratios (y) were plotted against the concentration ratios (x) of the standards of the target compounds to the internal standards. As illustrated in Table S1, satisfactory correlation coefficients ($R^2 \geq 0.9932$) were obtained within the range of 20.0 ~ 400.0 mg/L for ethyl pentanoate, 1000.0 ~ 20000.0 mg/L for ethyl hexanoate, 1.0 ~ 60.0 for propyl hexanoate, butyl hexanoate and hexyl hexanoate, and 5.0 ~ 80.0 mg/L for ethyl octanoate. Moreover, the LODs based on S/N = 3 were found to be 0.08 ~ 1.35 μg/L, while the LOQs (S/N = 10) were from 0.25 ~ 4.50 μg/L. The recovery studies were applied to evaluate the accuracy and precision with two spiking concentrations for OAEs in SAB samples (shown in Table S1). The results indicated that the average recoveries of ethyl hexanoate, butyl hexanoate, ethyl octanoate, and hexyl hexanoate were in the range of 70.1% ~ 90.0%, with relative standard deviations (RSDs, n = 3) from 2.0 to 9.8%.

In addition, a comparative study of the present method with other reported methods for the determination of six OAEs in different Baijiu and wine samples is demonstrated in Table 2. It can be seen that the accuracy and precision of the proposed method are comparable to those of previous methods. Moreover, the LODs of the method are lower or comparable to that of other techniques duo to the high surface area of synthesized GO/PAM/Fe_3O_4. Based on a comparison of the extraction time, the current method is greatly shorter than that of the most existing methods, which indicate that our method is more rapid and cost-effective. Therefore, the GO/PAM/Fe_3O_4 based MSPE method demonstrated a high potential for analyzing trace ester compounds from Baijiu

Table 2
Comparison of the proposed method with other reported methods in the determination of OAEs from different samples.

Analytical method	Sample Matrix	Organic solvent consumption	Extraction time (min)	LOD (μg/L)	Recoveries (%)	RSDs	Ref.
LLE-GC–MS	Gujinggong Baijiu	360 mL of CH_2Cl_2	240.0	3.8 ~ 43.5	85.0 ~ 104.0	1.0 ~ 4.4	(Zhao et al., 2018)
LLE-GC–MS	Langyatai Baijiu	150 mL of CH_2Cl_2	240.0	0.4 ~ 5.3	85.0 ~ 97.0	0.5 ~ 19.9	(Du et al., 2021)
SPME-GC–MS	Daohuaxiang Baijiu	100 mL of anhydrous diethyl ether	70.0	0.3 ~ 0.6	89.0 ~ 96.1	8.8 ~ 10.2	(Wang, Li, Qi, Li, & Pan, 2015)
SPME-GC–MS	Wine	——	25.0	5.8 ~ 7.2	93.0 ~ 101.0	4.6 ~ 11.5	(Paula Barros, Moreira, Elias Pereira, Leite, Moraes Rezende, & Guedes de Pinho, 2012)
SBSE-GC–MS	Sherry brandy	——	100.0	8.5 ~ 158.0	101.0 ~ 108.0	5.6 ~ 17.9	(Delgado, Durán, Castro, Natera, & Barroso, 2010)
SPE-GC–MS	Wine	1.3 mL CH_2Cl_2	35.0	0.2 ~ 0.3	85.0 ~ 90.0	6.3 ~ 9.2	(Andujar-Ortiz, Moreno-Arribas, Martín-Álvarez, & Pozo-Bayón, 2009)
MSPE-GC/MS	Luzhoulaojiao Baijiu	0.5 mL of CCl_4	15.0	0.08 ~ 1.35	70.1 ~ 90.0	2.0 ~ 9.8	In this work

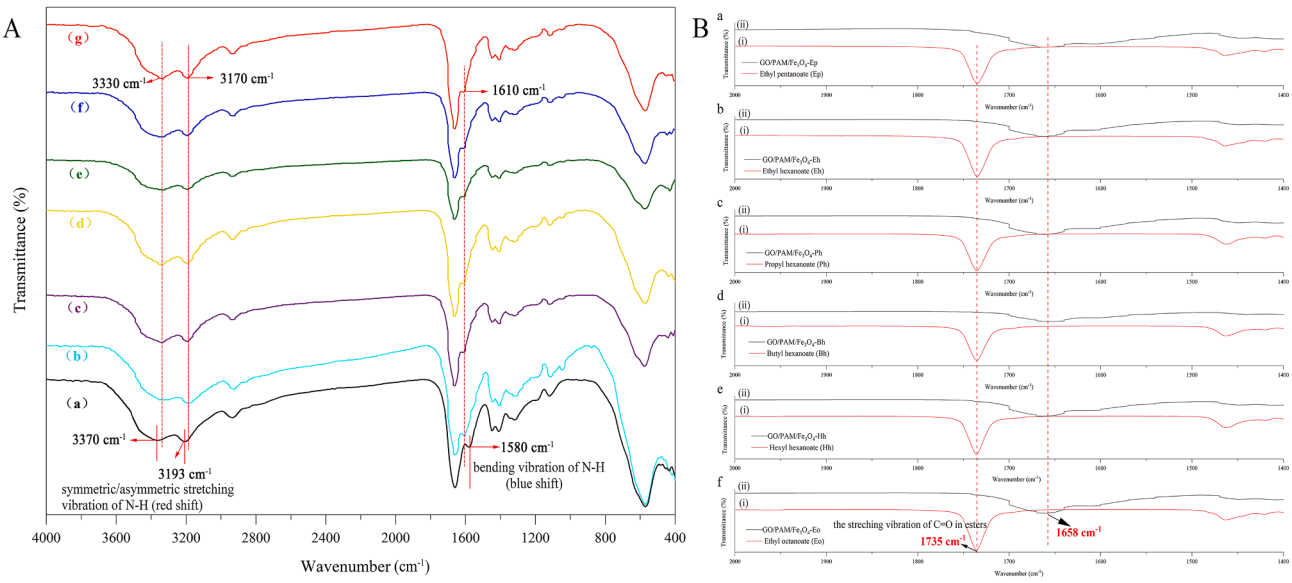

Fig. 3. (A) The FT-IR spectra of GO/PAM/Fe_3O_4 before (a) and after loading (b) ethyl pentanoate, (c) ethyl hexanoate, (d) propyl hexanoate, (e) butyl hexanoate, (f) hexyl hexanoate, and (g) ethyl octanoate; (B) The FT-IR spectra of six OAEs before (in red) and after (in black) adsorbed by GO/PAM/Fe_3O_4 in the 1400–2000 cm^{-1} region.

samples.

Application to real SAB samples

To further evaluate the applicability of the established MSPE-GC/MS method for the analysis of actual samples, five types of SAB samples obtained from Luzhoulaojiao Distillery Co., Ltd. were analyzed. Chromatograms of the spiked and unspiked real SAB extracts (at 20.0 mg/L of each analyte) treated with GO/PAM/Fe_3O_4 are also shown in Fig. S6. As shown in Table 3, ethyl pentanoate, ethyl hexanoate, propyl hexanoate, butyl hexanoate, ethyl octanoate, and hexyl hexanoate could be accurately quantified in all the SAB samples, with concentrations ranging from 28.6 ~ 105.2 mg/L, 1471.3 ~ 9080.5 mg/L, 2.3 ~ 7.5 mg/L, 7.0 ~ 22.5 mg/L, 17.0 ~ 56.4 mg/L, and 4.4 ~ 38.4 mg/L, respectively. Furthermore, to obtain deep insight into the contribution of these esters in the five SAB samples, their OAVs were also detected. Among them, ethyl hexanoate was calculated to have the highest OAV (29142 ~ 164115), followed by ethyl octanoate (OAV 1319 ~ 4383), ethyl pentanoate (OAV 1068 ~ 3972), butyl hexanoate (OAV 10 ~ 33), hexyl hexanoate (OAV 2 ~ 20) and propyl hexanoate (OAV 0.2 ~ 1). Therefore, except for propyl hexanoate, the other five OAEs (with OAVs higher than 1) were verified as important aroma compounds in the SAB samples responsible for the fruity, floral and sweet notes, which is consistent with the results described by numerous researchers (detailed in Table S3). Overall, the results demonstrated that the proposed method based on GO/PAM/Fe_3O_4 coupled with GC–MS exhibits accuracy and reliability for the selective recognition and extraction of OAEs from real Baijiu samples.

Conclusions

In the present study, by coupling the MSPE technique with GC–MS, a rapid, accurate and cost-effective method for the determination of OAEs in SAB samples was developed for the first time. The as-prepared GO/PAM/Fe_3O_4 exhibited highly selective recognition properties to esters, which attributed to the strong H-bonding interaction between the active sites of six OAEs and the amine groups and hydroxyls groups of GO/PAM/Fe_3O_4. Based on the results of adsorption experiments, Langmuir isotherm and pseudo-second-order models could best describe the adsorption with a maximum capacity ranging from 13.68 to 39.06 mg/g and a short equilibrium time of 15 min. Under the optimized MSPE conditions, the proposed method exhibited satisfactory recoveries in the

Table 3
Concentrations of six OAEs in 5-SAB determined by GO/PAM/Fe_3O_4-Based MSPE-GC/MS.

NO.	Ester odorants	SAB-1 * MC ± SD mg/L	RSD n = 3, %	SAB-2 MC ± SD mg/L	RSD n = 3, %	SAB-3 MC ± SD mg/L	RSD n = 3, %	SAB-4 MC ± SD mg/L	RSD n = 3, %	SAB-5 MC ± SD mg/L	RSD n = 3, %	[a] OT (μg/L)	OAV
1	Ethyl pentanoate	71.5 ± 1.5	2.1	28.6 ± 0.1	0.3	66.5 ± 0.9	1.4	59.6 ± 0.1	0.2	105.2 ± 0.7	0.7	26.8[b]	1068–3972
2	Ethyl hexanoate	9080.5 ± 323.0	3.6	8524.3 ± 281.3	3.3	1471.3 ± 77.2	5.2	1612.4 ± 59.6	3.7	5522.5 ± 5.7	0.1	55.3[b]	29142–164115
3	Propyl hexanoate	7.5 ± 0.1	1.3	2.8 ± 0.1	3.6	2.3 ± 0.1	4.3	2.3 ± 0.1	4.3	5.8 ± 0.1	1.7	12800.0[b]	0.2–1
4	Butyl hexanoate	22.5 ± 0.1	0.4	9.3 ± 0.1	1.1	7.0 ± 2.0 × 10^{-2}	0.3	7.1 ± 4.0 × 10^{-2}	0.6	20.9 ± 0.2	1.0	678.0[b]	10–33
5	Ethyl octanoate	33.1 ± 0.3	0.9	17.0 ± 0.2	1.2	24.7 ± 0.2	0.8	18.6 ± 0.1	0.5	56.4 ± 0.5	0.9	12.9[c]	1319–4383
6	Hexyl hexanoate	28.2 ± 0.3	1.1	8.9 ± 0.3	3.4	5.1 ± 4.0 × 10^{-2}	0.8	4.4 ± 0.1	2.3	38.4 ± 0.2	0.5	1890.0[d]	2–20

* MC ± SD = Mean Concentration ± standard deviations; [a] OT = Odor Threshold; [b] Odor threshold reported in (Fan & Xu, 2011); [c] Odor threshold reported in (Gao, Fan, & Xu, 2014); [d] Odor threshold reported in (Dong et al., 2019).

range of 70.1% ~ 90.0%, with RSDs from 2.0 to 9.8%. In addition to easier sample preparation process, the LOD and LOQ of 0.08 ~ 1.35 μg/L and 0.25 ~ 4.50 μg/L, respectively, were achieved, which were comparable or superior to the reported methods. Finally, the developed method was successfully applied in the analysis of six OAEs in real SAB samples. Overall, the newly developed MSPE-GC/MS assay has a potential to be a useful alternative to existing quantitative determination procedures for OAEs analysis.

CRediT authorship contribution statement

Ling Ao: Methodology, Validation, Formal analysis, Investigation, Writing – original draft. **Xudong Lian:** Methodology, Validation, Data curation, Writing – original draft. **Wenxuan Lin:** Methodology, Validation, Formal analysis, Investigation, Writing – original draft. **Ruonan Guo:** Methodology, Validation, Formal analysis, Investigation, Writing – original draft. **Youqiang Xu:** Writing – review & editing, Visualization. **Wei Dong:** Conceptualization, Methodology, Validation, Data curation, Supervision, Writing – review & editing. **Miao Liu:** Investigation, Resources, Supervision. **Caihong Shen:** Supervision, Writing – review & editing. **Xiaotao Sun:** Conceptualization, Supervision, Visualization, Writing – review & editing. **Baoguo Sun:** Supervision, Writing – review & editing. **Bo Deng:** Investigation, Resources.

Declaration of Competing Interest

The authors declare that they have no known competing financial interests or personal relationships that could have appeared to influence the work reported in this paper.

Acknowledgements

The work was supported by the National Natural Science Foundation of China (32102122), Department of Science and Technology of Sichuan Province (2019YFS0520 and 2021ZYD0102), National Engineering Research Center of Solid-state Brewing of Luzhoulaojiao Distillery Co., Ltd, and the Research Foundation for Youth Scholars of Beijing Technology and Business University (QNJJ2021-08).

Appendix A. Supplementary data

Supplementary data to this article can be found online at https://doi.org/10.1016/j.fochx.2022.100379.

References

Andujar-Ortiz, I., Moreno-Arribas, M. V., Martín-Álvarez, P. J., & Pozo-Bayón, M. A. (2009). Analytical performance of three commonly used extraction methods for the gas chromatography–mass spectrometry analysis of wine volatile compounds. *Journal of Chromatography A, 1216*(43), 7351–7357. https://doi.org/10.1016/j.chroma.2009.08.055

Cheng, M.-M., Huang, L.-J., Wang, Y.-X., Zhao, Y.-C., Tang, J.-G., Wang, Y., … Wickramasinghe, S. R. (2019). Synthesis of graphene oxide/polyacrylamide composite membranes for organic dyes/water separation in water purification. *Journal of Materials Science, 54*(1), 252–264. https://doi.org/10.1007/s10853-018-2828-9

Delgado, R., Durán, E., Castro, R., Natera, R., & Barroso, C. G. (2010). Development of a stir bar sorptive extraction method coupled to gas chromatography-mass spectrometry for the analysis of volatile compounds in Sherry brandy. *Analytica Chimica Acta, 672*(1), 130–136. https://doi.org/10.1016/j.aca.2010.05.015

Dong, C., Lu, J., Qiu, B., Shen, B., Xing, M., & Zhang, J. (2018). Developing stretchable and graphene-oxide-based hydrogel for the removal of organic pollutants and metal ions. *Applied Catalysis B: Environmental, 222*, 146–156. https://doi.org/10.1016/j.apcatb.2017.10.011

Dong, W., Guo, R., Liu, M., Shen, C., Sun, X., Zhao, M., Sun, J., Li, H., Zheng, F., Huang, M., & Wu, J. (2019). Characterization of key odorants causing the roasted and mud-like aromas in strong-aroma types of base Baijiu. *Food Research International, 125*, Article 108546. https://doi.org/10.1016/j.foodres.2019.108546

Du, J., Li, Y., Xu, J., Huang, M., Wang, J., Chao, J., Wu, J., Sun, H., Ding, H., & Ye, H. (2021). Characterization of key odorants in Langyatai Baijiu with Jian flavour by sensory-directed analysis. *Food Chemistry, 352*, Article 129363. https://doi.org/10.1016/j.foodchem.2021.129363

Fan, W., & Xu, Y. (2011). Determination of Odor Thresholds of Volatile Aroma Compounds in Baijiu by A Forced-choice Ascending Concentration Series Method of Limits. *Liquor Making, 38*, 80–84. in Chinese.

Filho, E., Brito, E., Silva, R., Streck, L., Bohn, F., & Fonseca, J. (2021). Superparamagnetic polyacrylamide/magnetite composite gels. *Journal of Dispersion Science and Technology, 42*(10), 1504–1512. https://doi.org/10.1080/01932691.2020.1774382

Fraga, T. J. M., de Souza, Z. S. B., Marques Fraga, D. M. d. S., Carvalho, M. N., de Luna Freire, E. M. P., Ghislandi, M. G., & da Motta Sobrinho, M. A. (2020). Comparative approach towards the adsorption of Reactive Black 5 and methylene blue by n-layer graphene oxide and its amino-functionalized derivative. *Adsorption, 26*(2), 283-301. https://doi.org/10.1007/s10450-019-00156-9.

Gao, W., Fan, W., & Xu, Y. (2014). Characterization of the Key Odorants in Light Aroma Type Chinese Liquor by Gas Chromatography-Olfactometry, Quantitative Measurements, Aroma Recombination, and Omission Studies. *Journal of Agricultural and Food Chemistry, 62*(25), 5796–5804. https://doi.org/10.1021/jf501214c

Guo, L., Ma, X., Xie, X., Huang, R., Zhang, M., Li, J., Zeng, G., & Fan, Y. (2019). Preparation of dual-dummy-template molecularly imprinted polymers coated magnetic graphene oxide for separation and enrichment of phthalate esters in water. *Chemical Engineering Journal, 361*, 245–255. https://doi.org/10.1016/j.cej.2018.12.076

He, X., Yangming, H., Górska-Horczyczak, E., Wierzbicka, A., & Jeleń, H. H. (2021). Rapid analysis of Baijiu volatile compounds fingerprint for their aroma and regional origin authenticity assessment. *Food Chemistry, 337*, Article 128002. https://doi.org/10.1016/j.foodchem.2020.128002

Hu, L., Yang, Z., Cui, L., Li, Y., Ngo, H. H., Wang, Y., Wei, Q., Ma, H., Yan, L., & Du, B. (2016). Fabrication of hyperbranched polyamine functionalized graphene for high-efficiency removal of Pb(II) and methylene blue. *Chemical Engineering Journal, 287*, 545–556. https://doi.org/10.1016/j.cej.2015.11.059

Karbalaie, B., Rajabi, M., & Fahimirad, B. (2020). Dopamine-modified magnetic graphene oxide as a recoverable sorbent for the preconcentration of metal ions by an effervescence-assisted dispersive micro solid-phase extraction procedure. *Analytical Methods, 12*(18), 2338–2346. https://doi.org/10.1039/D0AY00522C

Li, M., Feng, J., Huang, K., Tang, S., Liu, R., Li, H., Ma, F., & Meng, X. (2019). Amino group functionalized SiO2@graphene oxide for efficient removal of Cu(II) from aqueous solutions. *Chemical Engineering Research and Design, 145*, 235–244. https://doi.org/10.1016/j.cherd.2019.03.028

Liang, W., Lu, Y., Li, N., Li, H., & Zhu, F. (2020). Microwave-assisted synthesis of magnetic surface molecular imprinted polymer for adsorption and solid phase extraction of 4-nitrophenol in wastewater. *Microchemical Journal, 159*, Article 105316. https://doi.org/10.1016/j.microc.2020.105316

Liu, H., & Sun, B. (2018). Effect of Fermentation Processing on the Flavor of Baijiu. *Journal of Agricultural and Food Chemistry, 66*(22), 5425–5432. https://doi.org/10.1021/acs.jafc.8b00692

Lu, T., Xue, C., Shao, J., Gu, J.-D., Zeng, Q., & Luo, S. (2016). Adsorption of dibutyl phthalate on Burkholderia cepacia, minerals, and their mixtures: Behaviors and mechanisms. *International Biodeterioration & Biodegradation, 114*, 1–7. https://doi.org/10.1016/j.ibiod.2016.05.015

Lu, Z., Yu, J., Zeng, H., & Liu, Q. (2017). Polyamine-modified magnetic graphene oxide nanocomposite for enhanced selenium removal. *Separation and Purification Technology, 183*, 249–257. https://doi.org/10.1016/j.seppur.2017.04.010

Manousi, N., Deliyanni, E. A., Rosenberg, E., & Zachariadis, G. A. (2021). Ultrasound-assisted magnetic solid-phase extraction of polycyclic aromatic hydrocarbons and nitrated polycyclic aromatic hydrocarbons from water samples with a magnetic polyaniline modified graphene oxide nanocomposite. *Journal of Chromatography A, 1645*, Article 462104. https://doi.org/10.1016/j.chroma.2021.462104

Nazir, M. A., Bashir, M. A., Najam, T., Javed, M. S., Suleman, S., Hussain, S., Kumara, O. P., Ahmad Shah, S. S., Rehman, A., & u. (2021). Combining structurally ordered intermetallic nodes: Kinetic and isothermal studies for removal of malachite green and methyl orange with mechanistic aspects. *Microchemical Journal, 164*, Article 105973. https://doi.org/10.1016/j.microc.2021.105973

Niu, Y., Yu, D., Xiao, Z., Zhu, J., Song, S., & Zhu, G. (2015). Use of Stir Bar Sorptive Extraction and Thermal Desorption for Gas Chromatography-Mass Spectrometry Characterization of Selected Volatile Compounds in Chinese Liquors. *Food Analytical Methods, 8*(7), 1771–1784. https://doi.org/10.1007/s12161-014-0060-z

Paula Barros, E., Moreira, N., Elias Pereira, G., Leite, S. G. F., Moraes Rezende, C., & Guedes de Pinho, P. (2012). Development and validation of automatic HS-SPME with a gas chromatography-ion trap/mass spectrometry method for analysis of volatiles in wines. *Talanta, 101*, 177–186. https://doi.org/10.1016/j.talanta.2012.08.028

Peng, S., Zhang, D., Huang, H., Jin, Z., & Peng, X. (2019). Ionic polyacrylamide hydrogel improved by graphene oxide for efficient adsorption of methylene blue. *Research on Chemical Intermediates, 45*(3), 1545–1563. https://doi.org/10.1007/s11164-018-3689-1

Ploychompoo, S., Liang, Q., Zhou, X., Wei, C., & Luo, H. (2021). Fabrication of Zn-MOF-74/polyacrylamide coated with reduced graphene oxide (Zn-MOF-74/rGO/PAM) for As(III) removal. *Physica E: Low-dimensional Systems and Nanostructures, 125*, Article 114377. https://doi.org/10.1016/j.physe.2020.114377

Pourjavadi, A., Nazari, M., Kohestanian, M., & Hosseini, S. H. (2019). Polyacrylamide-grafted magnetic reduced graphene oxide nanocomposite: Preparation and adsorption properties. *Colloid and Polymer Science, 297*(6), 917–926. https://doi.org/10.1007/s00396-019-04506-5

Senosy, I. A., Guo, H.-M., Ouyang, M.-N., Lu, Z.-H., Yang, Z.-H., & Li, J.-H. (2020). Magnetic solid-phase extraction based on nano-zeolite imidazolate framework-8-functionalized magnetic graphene oxide for the quantification of residual fungicides

in water, honey and fruit juices. *Food Chemistry, 325*, Article 126944. https://doi.org/10.1016/j.foodchem.2020.126944

Sun, B. (2021). *Chinese National Alcohols: Baijiu and Huangjiu.* Beijing, China: World Scientific Publishing Co., Pte. Ltd.

Viana, M. M., do Amparo, S. Z. S., Lima, M. C. F. S., Lopes, R. C. F. G., Vasconcelos, C. K. B., Caliman, V., & Silva, G. G. (2020). Microwave-assisted synthesis of polyacrylamide-aminated graphene oxide hybrid hydrogel with improved adsorption properties. *Journal of Environmental Chemical Engineering, 8*(5), 104415. https://doi.org/10.1016/j.jece.2020.104415.

Wang, P.-P., Li, Z., Qi, T.-T., Li, X.-J., & Pan, S.-Y. (2015). Development of a method for identification and accurate quantitation of aroma compounds in Chinese Daohuaxiang liquors based on SPME using a sol–gel fibre. *Food Chemistry, 169*, 230–240. https://doi.org/10.1016/j.foodchem.2014.07.150

Wang, J., Chen, H., Wu, Y., & Zhao, D. (2022). Uncover the flavor code of strong-aroma baijiu: Research progress on the revelation of aroma compounds in strong-aroma baijiu by means of modern separation technology and molecular sensory evaluation. *Journal of Food Composition and Analysis, 109*, 104499. https: //doi.org/10.1016/j.jfca.2022.104499.

Xiao, R., Zhang, X., Zhang, X., Niu, J., Lu, M., Liu, X., & Cai, Z. (2017). Analysis of flavors and fragrances by HPLC with Fe3O4@GO magnetic nanocomposite as the adsorbent. *Talanta, 166*, 262–267. https://doi.org/10.1016/j.talanta.2017.01.065

Xu, Y., Zhao, J., Liu, X., Zhang, C., Zhao, Z., Li, X., & Sun, B. (2022). Flavor mystery of Chinese traditional fermented baijiu: The great contribution of ester compounds. *Food Chemistry, 369*, Article 130920. https://doi.org/10.1016/j.foodchem.2021.130920

Yin, S., Yang, Y., Yang, D., Li, Y.-X., Jiang, Y., Wu, L., & Sun, C. (2019). Determination of 11 Phthalate Esters in Beverages by Magnetic Solid-Phase Extraction Combined with High Performance Liquid Chromatography. *Journal of Aoac International, 102*. https://doi.org/10.5740/jaoacint.18-0316

Zhan, C.-G., Landry, D. W., & Ornstein, R. L. (2000). Energy Barriers for Alkaline Hydrolysis of Carboxylic Acid Esters in Aqueous Solution by Reaction Field Calculations. *The Journal of Physical Chemistry A, 104*(32), 7672–7678. https://doi.org/10.1021/jp001459i

Zhang, Q., Liu, G., Cao, X., Yin, J., & Zhang, Z. (2020). Preparation of magnetic zeolitic imidazolate framework-67 composites for the extraction of phthalate esters from environmental water samples. *Analytical Methods, 12*(40), 4906–4912. https://doi.org/10.1039/D0AY01482F

Zhao, D., Shi, D., Sun, J., Li, A., Sun, B., Zhao, M., Chen, F., Sun, X., Li, H., Huang, M., & Zheng, F. (2018). Characterization of key aroma compounds in Gujinggong Chinese Baijiu by gas chromatography–olfactometry, quantitative measurements, and sensory evaluation. *Food Research International, 105*, 616–627. https://doi.org/10.1016/j.foodres.2017.11.074